Semibatch Bubble-Column Slurry Reactors: Effects of Dispersion on the Steady-State Behavior

V. M. H. GOVINDARAO and
M. CHIDAMBARAM

Department of Chemical Engineering
Indian Institute of Science
Bangalore-560012, India

INTRODUCTION

Bubble-column slurry reactors (BCSR) are used extensively for gas-liquid-solid contacting in chemical and petroleum industries, and in pollution control. Østergaard (1968), Shah (1979), Hammer (1979), and Chaudhari and Ramachandran (1980) presented excellent reviews of the work done on these reactors. Though distribution of the concentration, particularly of the solid particles in the slurry systems, is known to be significant, not much work is reported on its effect on the behavior of the slurry reactors. Govindarao (1975a) has suggested the use of dispersion model for the gas and the liquid phases, and sedimentation-diffusion model for the solid phase, and evaluated the behavior of a semibatch BCSR by analog simulation (1975b).

Here, the steady-state profiles were obtained as the time tending to ∞ solution of the dynamic model, and effects of dispersion in the phases were not evaluated in detail. Recently Deckwer et al. (1982) reported the application of the dispersion model to Fischer-Tropsch synthesis in slurry phase. In this paper, the dispersion model applied to the steady-state operation of a BCSR (with first-order surface reaction) is solved analytically. The effect of mixing in the different phases is evaluated numerically.

MODEL EQUATIONS AND SOLUTION

For isothermal and steady-state operation, the semibatch BCSR with a first-order surface reaction is modelled (Govindarao, 1975a) by the following equations:

$$\frac{1}{Pe_G}\frac{d^2C_1}{dZ^2} - \frac{dC_1}{dZ} - \frac{N_1}{m_1}(C_1 - C_2) = 0 \tag{1}$$

$$\frac{1}{Pe_{GL}}\frac{d^2C_2}{dZ^2} + N_1\phi(C_1 - C_2) - M_1f(C_2 - C_3) = 0 \tag{2}$$

$$M_1f(C_2 - C_3) - QfCn3 = 0 \tag{3}$$

$$f = \exp(-Pe_pZ) \tag{4}$$

The associated boundary conditions are:

$$\left.\frac{dC_1}{dZ}\right|_{Z=0} = Pe_G\left(C_1\big|_{Z=0} - 1\right); \quad \left.\frac{dC_1}{dZ}\right|_{Z=1} = 0 \tag{5a}$$

$$\left.\frac{dC_2}{dZ}\right|_{Z=0} = 0; \quad \left.\frac{dC_2}{dZ}\right|_{Z=1} = 0 \tag{5b}$$

This model considers, in particular, the experimental observation (Imafuku et al., 1968; Kato et al., 1972) that, for the particle sizes, particle loadings and gas flow rates of interest in a BCSR, the axial dispersion coefficient of the particles and the liquid are equal.

From Eq. 3 we get,

$$C_3 = \frac{M_1}{(M_1 + Q)}C_2 \tag{6}$$

Combining Eqs. 1 to 3 to eliminate C_1 and C_3 we get the following fourth-order, linear, variable-coefficient, ordinary differential equation in C_2:

$$\frac{d^4C_2}{dZ^4} - Pe_G\frac{d^3C_2}{dZ^3} - (a_1f + a_2)\frac{d^2C_2}{dZ^2} + (a_3f + a_4)\frac{dC_2}{dZ} - a_5fC_2 = 0 \tag{7}$$

The above equation is solved here by series-solution method suggested by Kaplan (1962). It is first converted into the standard form (Kaplan, 1962) by transforming the indpendent variable Z to f where f is given by Eq. 4. Then by substituting $C_2 = f^\alpha$, and equating the coefficient of f^α in the resulting equation to zero, we get the following indicial equation:

$$\alpha\left[\alpha^3 + a_{12}\alpha^2 - a_6\alpha - \frac{a_4}{P_{eP}^3}\right] = 0 \tag{8}$$

If α_1, α_2, α_3 and α_4 are the roots of this equation, the general solution of Eq. 7 is given by

$$C_2 = \sum_{i=1}^{4} y_iX_i \tag{9}$$

where

$$X_i = \exp(-\alpha_iPe_PZ)\sum_{j=0}^{\infty} b_{ij}\exp(-jPe_PZ) \tag{10}$$

and y_1 to y_4 are calculated from the boundary conditions, Eqs. 5, and are given by the solution of the equation

$$Ay = J \tag{11}$$

with the matrix A and the vector J as given in the Appendix. The quantities b_{ij} are given by the recurrence relation:

$$b_{ij} = \frac{\left[\frac{a_5}{P_{eP}^4} + a_{11}(\alpha_i + j - 1) + a_9(\alpha_i + j - 1)(\alpha_i + j - 2)\right]}{\begin{aligned}&(\alpha_i + j)[(\alpha_i + j - 1)(\alpha_i + j - 2)(\alpha_i + j - 3) \\ &\times b_{i(j-1)} + a_7(\alpha_i + j - 1)(\alpha_i + j - 2) \\ &\qquad + a_8(\alpha_i + j - 1) + a_{10}]\end{aligned}} \tag{12}$$

where $b_{i0} = 1$, $i = 1$ to 4 and $j = 1$ to ∞. From Eqs. 2, 6, and 9, we get for C_1:

$$C_1 = \sum_{i=1}^{4} y_i\left(SX_i - \frac{1}{Pe_{GL}N_1\phi}\frac{d^2X_i}{dZ^2}\right) \tag{13}$$

where

$$S = \left[1 + \left(\frac{M_1Q}{M_1 + Q}\right)\frac{f}{N_1\phi}\right] \tag{14}$$

C_3 is calculated from Eq. 6.

Once the operating conditions of a BCSR are known, α_i's are calculated from Eq. 8 and y_i's from Eq. 11. Then, C_1, C_2 and C_3 profiles are calculated from Eqs. 13, 9 and 6, respectively. These solutions apply to the general case, that is, with finite dispersion in the gas and the slurry phases. Solutions for special cases with different possible levels of mixing in each phase can be deduced from these equations by appropriate substitutions. Of particular interest is the operation of the reactor where feed gas is pure, such as in hydrogenation of organic liquids. Application of the model to one such example, the hydrogenation of α-methyl-styrene, is being discussed elsewhere.

NUMERICAL EVALUATION

The effects of mixing on the performance of the BCSR are numerically evaluated. Table 1 gives the operating conditions used for the purpose (Govindarao, 1975a).

TABLE 1. PARAMETERS USED FOR THE NUMERICAL EVALUATION

Pressure	1 atm
Temperature, T	298.1 K
Density of the gas, ρ_G	0.0823 g·L^{-1}
Density of the liquid, ρ_L	0.85 g·cm^{-3}
Viscosity of the liquid, μ_L	0.31 cP
Density of the particle, ρ_P	3.35 g·cm^{-3}
Bubble diameter	0.28 cm
Bubble rise velocity, U_G	21.74 cm·s^{-1}
Henry's law constant, H	3.876 × 10^5 atm·cm^3·gmol^{-1}
Gas-liquid mass transfer coefficient, k_a	2.544 × 10^{-2} cm·s^{-1}
Reactor length, L	200 cm
Diffusivity of the gas in the liquid	4.82 × 10^{-5} cm^2·s^{-1}
Gas phase Peclet number, Pe_G	0.005, 0.5, 5, 500
Superficial velocity of the gas, v_G	5 cm·s^{-1}
Catalyst loading, W	5, 10, 20, 40, 60, 80, 100, 200 g·L^{-1}
Particle diameter, d_p	10, 25, 50, 75, 100 μm
Reactor diameter, d_T	20 cm
Reactor rate constant, k_1	0.04 cm·s^{-1}

Figure 1 shows typical concentration profiles in each phase for several values of gas-phase and slurry-phase dispersion coefficients. The level of mixing in each phase has strong effect on the profiles, particularly on the profile in the liquid phase.

In the design and operation of slurry reactors an important quantity measuring its performance is the conversion of the gas component. Effects of catalyst loading and particle size on the conversion of the gas component at different levels of mixing in the gas and slurry phases are shown in Figure 2. The plots show very significant effect of the mixing conditions on the conversion. This indicates that for the design of slurry reactors for a desired conversion, choice of the catalyst loading, and the particle size is dictated by the disperion coefficient of the gas phase and slurry phase as well. For a given mixing condition in the gas and slurry phases, the conversion is higher for smaller particles and larger catalyst loadings. Also, the influence of gas-phase mixing on the conversion is more predominant at these conditions. Slurry-phase mixing affects the conversion strongly at higher catalyst loadings and larger particle diameters.

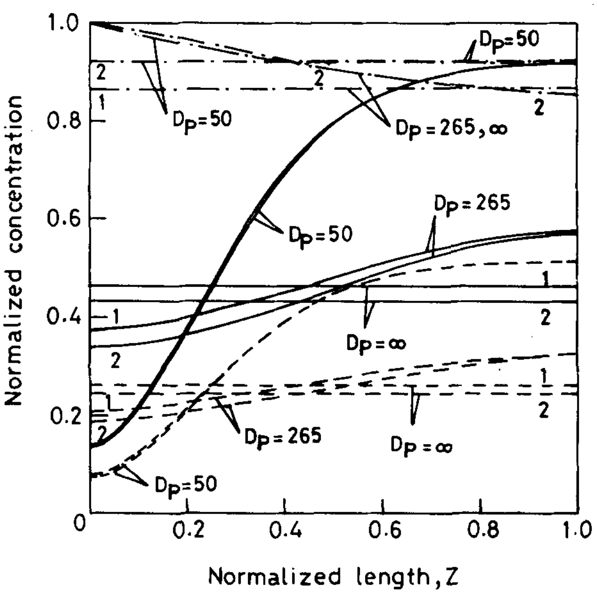

Figure 1. Effect of backmixing in the gas phase and slurry phase on the steady-state concentration profiles.

- · - · - · - · - C_1 | 1: Gas plug flow
———— C_2 | 2: Gas completely backmixed
- - - - - - C_3 |
W = 20 g/L; d_p = 50 μm;

other conditions as given in Table 1.

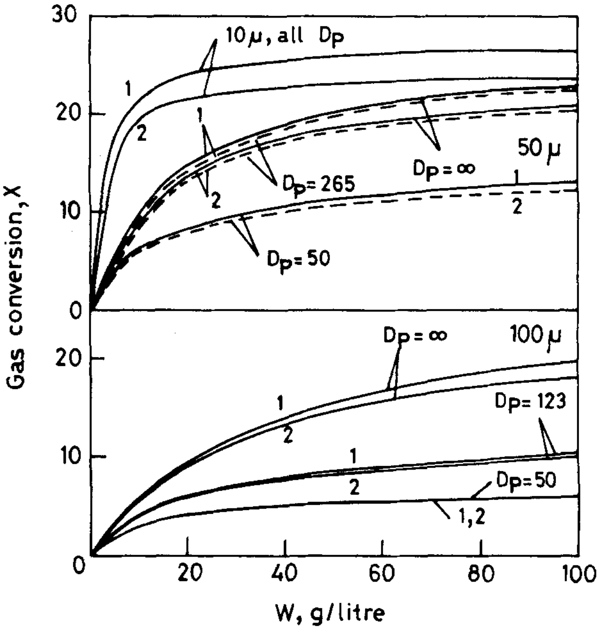

Figure 2. Effect of backmixing in the gas phase and slurry phase on the conversion vs. catalyst loading.

Figure 2 also includes curves corresponding to the particles dispersion coefficient D_p, estimated by using the correlation of Kato et al. (1972):

$$\frac{v_G d_T}{D_P} = -\frac{13\,Fr}{(1+8Fr^{0.85})}(1+0.009\,ReFr^{-0.8}) \qquad (15)$$

The correlation is likely to be valid for most practical systems, and the corresponding curves are, therefore, representative of the prevailing conditions in BCSR's. Figure 2 shows that, for small particle sizes under the conditions studied, increasing D_P from the value predicted by the correlation of Kato et al. has practically no influence on the conversion behavior (though the corresponding concentration profiles are affected significantly). This means that for low particle sizes, the slurry phase may be considered to be well

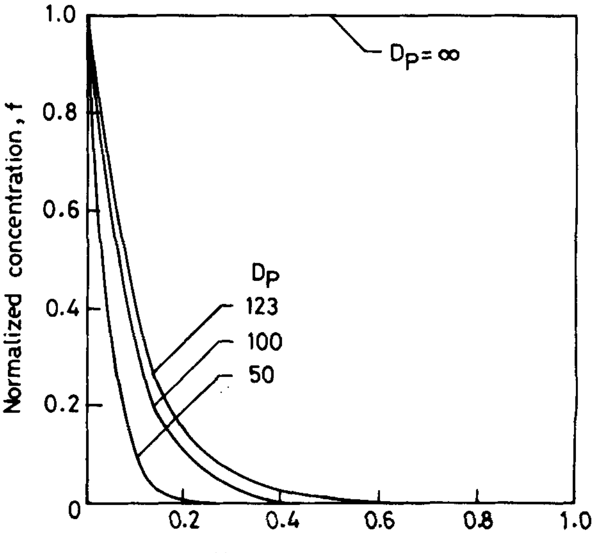

Figure 3. Concentration distribution of solid particles for different values of D_P.

d_P = 100 μm; other conditions as given in Table 1.

mixed. On the other hand, for higher particle diameters, the assumption is no more valid; the conversions are affected strongly as D_P is increased from the value corresponding to the correlation of Kato et al.

For a given d_P and W (higher ranges), the effect of mixing in gas phase is more significant at higher levels of mixing in the slurry phase than at lower levels. As catalyst loading increases the curves for different levels of mixing in the gas (or slurry phase) become approximately parallel to each other indicating that quantitatively the influence of mixing in a given phase reaches an essentially constant level with W.

It is also seen from Figure 2 that for a given W and d_P (higher values) conversion increases with D_P. This apparently anomalous behavior is due to the influence of the adverse concentration profile of the catalyst particles. As seen in Figure 3, for $D_P = 50$ cm^2/s which is already a relatively high value, the catalyst concentration virtually falls down to zero after a normalized reactor length of about 0.2. For this mixing condition in the slurry phase then, no reaction occurs in the remaining 80% of the reactor. The influence of the distribution of the catalyst particles can be seen more clearly by considering the fictitious proposition where the concentration of the solids is always uniform throughout the reactor. Then the conversion is approximately the same for very low as well as very high levels of mixing in the liquid phase. But, once the distribution of the particles is also taken into account, the conversion becomes very low for low levels of mixing. The discussion thus clearly indicates that the reactor behavior is strongly affected by the distribution of the solid particles. Govindarao (1975a) has found similar influence on the dynamics of the reactor also. Thus, the commonly-made assumption of well-mixed slurry phase in the BCSR is not generally valid.

We note from Eq. 4 that the catalyst concentration profile is influenced by any variable that affects the mean settling velocity of the particles, U_S, and/or the slurry-phase dispersion coefficient, D_P. Thus, it may be concluded that particle diameter, particle density, reactor dimensions, liquid-phase properties and gas velocity will all influence the effects of mixing on the performance of the BCSR. However, the effect of the gas velocity is perhaps less prominent since its influence on the w distribution is not very significant (Govindarao, 1975a).

The effect of gas-phase mixing on the conversion is almost negligible for higher particle sizes even at high catalyst loadings. Even at lower particle size, the effect is relatively small. For example, for $d_P = 10$ μm, and $W = 60$ g/L, the change in conversion for gas plug-flow to gas well-mixed condition is only from 0.26 to 0.23. Furthermore, for the most situations, in practice,the commonly-made assumption of plug flow in the gas phase is quite valid.

CONCLUSIONS

Based on the dispersion model for each phase of a semibatch BCSR, analytical solutions are derived for the steady-state axial concentration profiles of the diffusing component. Numerical evaluation of the model shows that mixing in the gas and slurry phases affects the behavior of the reactor very significantly. The influence of mixing on gas-phase conversion versus catalyst loading and particle size provides important characteristics for the design of the reactor. Effect of slurry-phase dispersion is more significant at higher catalyst loadings and larger particle diameters, while effect of gas-phase dispersion is more significant at higher catalyst loadings and smaller particle diameters.

Conversion increases with increasing mixing in the slurry phase, the well-mixed slurry phase giving the highest conversion, because of the effect of the concentration profile of the catalyst particles. Thus, the conditions that give more uniform distribution of the solid particles, such as lower particle diameters, larger reactor diameters, lighter particles, higher gas velocities, etc., result in higher conversions. The results also indicate that the commonly-made assumption of well-mixed slurry phase is not generally valid, while the assumption of plug flow in the gas phase is quite adequate for most situations.

NOTATION

A = matrix defined in the Appendix
a = surface area of gas bubbles per unit volume of the gas, cm^2·cm^{-3}
a_w = particle surface area per unit weight, cm^2·g^{-1}
a_1 = $(M_1 Q Pe_{GL})/(M_1 + Q)$
a_2 = $(Pe_{GL} N_1 \phi + Pe_G N_1/m_1)$
a_3 = $a_1(2Pe_P + Pe_G)$
a_4 = $Pe_G Pe_{GL} N_1 \phi$
a_5 = $a_1(P_{eP}^2 + Pe_G Pe_P - Pe_G N_1/m_1)$
a_6 = a_2/P_{eP}^2
a_7 = $6 + a_{12}$
a_8 = $7 - a_6 + 3a_{12}$
a_9 = a_1/P_{eP}^2
a_{10} = $1 + a_{12} - a_6 - a_4/P_{eP}^3$
a_{11} = $a_9 + a_3/P_{eP}^3$
a_{12} = Pe_G/Pe_P
b_{ij} = coefficient defined by Eq. 12
C = concentration of the diffusing component, gmol·cm^{-3}

APPENDIX

$$A = \begin{bmatrix} \left.\frac{dX_1}{dZ}\right|_0 & \left.\frac{dX_2}{dZ}\right|_0 & \left.\frac{dX_3}{dZ}\right|_0 & \left.\frac{dX_4}{dZ}\right|_0 \\ \left.\frac{dX_1}{dZ}\right|_1 & \left.\frac{dX_2}{dZ}\right|_1 & \left.\frac{dX_3}{dZ}\right|_1 & \left.\frac{dX_4}{dZ}\right|_1 \\ E_1|1 & E_2|_1 & E_3|1 & E_4|_1 \\ V_1 & V_2 & V_3 & V_4 \end{bmatrix} ; J = \begin{bmatrix} 0 \\ 0 \\ 0 \\ -Pe_G \end{bmatrix}$$

where

$$E_i = \left[S \frac{dX_i}{dZ} - \frac{1}{Pe_{GL} N_1 \phi} \frac{d^3 X_i}{dZ^3} - \frac{f}{N_1 \phi} Pe_P \left(\frac{M_1 Q}{M_1 + Q} \right) X_i \right]$$

and

$$V_i = E_i|_{Z=0} - Pe_G \left[X_i S - \frac{1}{Pe_{GL} N_1 \phi} \frac{d^2 X_i}{dZ^2} \right]_{Z=0}; \quad i = 1 \text{ to } 4.$$

C_1 = $C_G/\overline{C}_G^o$, normalized concentration in the gas phase
C_2 = $m_1C_L/\overline{C}_G^o$, normalized concentration in the liquid phase
C_3 = $m_1C_S/\overline{C}_G^o$, normalized concentration on the surface of the particles
$\overline{C}_G^o$ = concentration of the diffusing component in the entering gas phase, gmol·cm^{-3}
D = axial dispersion coefficient, cm^2·s^{-1}
d_p = diameter of the particles, cm
d_T = reactor diameter, cm
E_i = defined in the Appendix
Fr = $v_G/(gd_T)^{1/2}$, Froude number
f = $w/(W\tau)$, normalized concentration of the particles
g = acceleration due to gravity, cm^2·s^{-1}
H = Henry's law constant, cm^3·atm·gmol^{-1}
J = column vector defined in the Appendix
k = mass transfer coefficient, cm·s^{-1}
k_1 = surface reaction rate constant, cm·s^{-1}
L = length of the reactor, cm
M_1 = $k_ca_wWL\tau/U_G$
m_1 = H/RT
N_1 = k_aaL/U_G
Pe_G = U_GL/D_G, Peclet number of the gas phase
Pe_{GL} = U_GL/D_P
Pe_P = U_SL/D_P, Peclet number of the particles
Q = $k_1a_wWL\tau/U_G$
R = gas constant, cm^3·atm·gmol^{-1}·deg^{-1}
Re = $d_PU_t\rho_L/\mu_L$, particle Reynolds number
S = defined by Eq. 14
T = temperature, K
U_G = bubble rise velocity, cm·s^{-1}
U_S = mean settling velocity of the particles, cm·s^{-1}
U_t = particle terminal velocity, cm·s^{-1}
V_i = defined in the Appendix
v_G = superficial velocity of the gas, cm·s^{-1}
W = catalyst loading, g·cm^{-3}
W_L = catalyst loading, g/L of the reactor
w = concentration of the particles, g·cm^{-3}
X = gas phase conversion
X_i = defined by Eq. 10
y = vector $[y_1y_2y_3y_4]^T$
y_i = ith element of the vector y
Z = z/L, normalized height from the bottom of the column
z = height from the bottom of the column, cm

Greek Letters

α = variable of the indicial equation
α_1, α_2, α_3 and α_4 = indicial roots defined by Eq. 8
ϵ = fractional gas holdup
μ_L = viscosity of the liquid, cP
ρ = density, g·cm^{-3}
τ = $(U_SL/D_P)[1 - \exp(-U_SL/D_P)]^{-1}$
ϕ = $\epsilon/(1 - \epsilon)$

Subscripts

0 = at $Z = 0$
a = gas-liquid
c = fluid-particle
G = gas-phase
L = liquid phase
P = particle
S = particle surface

LITERATURE CITED

Chaudhari, R. V., and P. A. Ramachandran, "Three Phase Slurry Reactors," *AIChE J.*, **26**, 177 (1980).
Deckwer, W. D., Y. Serpeman, M. Ralek, and B. Schmidt, "Modelling the Fischer-Tropsch Synthesis in the Slurry Phase," *Ind. Eng. Chem. Process Des. Dev.*, **21**, 231 (1982).
Govindararo, V. M. H., "On Dynamics of Bubble Column Slurry Reactors," *Chem. Eng. J.*, **9**, 229 (1975a).
———, "Analog Simulation of an Isothermal Semibatch Bubble Column Slurry Reactor," *Ann. Asso. Int. Calc. Analogique.*, **2**, 69 (1975b).
Hammer, H., "Bubble Column Reactors with Suspended Solids: Fundamentals, Design and Uses," *Int. Chem. Eng.*, **21**, 173 (1981).
Imafuku, K., T. Wang, K. Koide, and H. Kuboda, "The Behaviour of Suspended Solid Particles in the Bubble Column," *J. Chem. Eng. Japan*, **1**, 153 (1968).
Kaplan, W., *Operational Methods for Linear Systems*, Addison-Wesley Pub. Co., 456 (1962).
Kato, Y., A. Nishiwaki, T. Fukuda, and S. Tanaka, "The Behaviour of Suspended Solid Particles and Liquid in Bubble Columns," *J. Chem. Eng. Japan.*, **5**, 112 (1972).
Østergaard, K., "Gas-Liquid-Particle Operations in Chemical Reaction Engineering," *Adv. Chem. Eng.*, **7**, 71 (1968).
Shah, Y. T., *Gas-Liquid-Solid Reactor Design*, McGraw-Hill, ABP (1979).

Manuscript received October 5, 1982; revision received February 8, and accepted February 28, 1983.

Use of Packed Rectification Columns in Extractive Distillation

LLOYD BERG,
P. RATANAPUPECH, and
A. I. YEH

Department of Chemical Engineering
Montana State University
Bozeman, MT

Can extractive distillation be carried out in a packed rectification column or must it always be done in plate columns. To answer this question, four different packings were evaluated with ten different extractive distillation agents in the separation of ethyl acetate from the ethyl acetate-ethanol-water mixture and compared with a perforated plate column. The results showed that the packed columns were not quite as efficient as the plate column and that they ranked in the order: glass helices, Berl saddles, Intalox saddles, and glass Raschig rings.